Springer Proceedings in Physics 141

Martin Oberlack
Joachim Peinke
Alessandro Talamelli
Luciano Castillo
Michael Hölling *Editors*

# Progress in Turbulence and Wind Energy IV

## Proceedings of the iTi Conference in Turbulence 2010

Springer

For further volumes:
http://www.springer.com/series/361

Editors

Martin Oberlack · Joachim Peinke ·
Alessandro Talamelli · Luciano Castillo ·
Michael Hölling

# Progress in Turbulence and Wind Energy IV

## Proceedings of the iTi Conference in Turbulence 2010

Springer

*Editors*
Prof. Dr. Martin Oberlack
Department of Mechanical
Engineering
Technische Universität Darmstadt
Darmstadt
Germany

Prof. Dr. Luciano Castillo
Mechanical, Aerospace & Nuclear
Engineering Department
Rensselaer Polytechnic Institute
Troy
USA

Prof. Dr. Joachim Peinke
Institute of Physics & ForWind
University Oldenburg
Oldenburg
Germany

Dr. Michael Hölling
Institute of Physics & ForWind
University of Oldenburg
Oldenburg
Germany

Prof. Dr. Alessandro Talamelli
II Facoltà di Ingegneria
Universita di Bologna
Forli
Italy

ISSN 0930-8989 e-ISSN 1867-4941
ISBN 978-3-642-28967-5 e-ISBN 978-3-642-28968-2
DOI 10.1007/978-3-642-28968-2
Springer Heidelberg New York Dordrecht London

Library of Congress Control Number: 2012934378



Printed on acid-free paper

Springer is part of Springer Science+Business Media (www.springer.com)

*“Allora è l’huomo in pace, quando per morte è uscito delle turbolenze di questo mondo, e venuto alla salute eterna.”*

*Prima definizione di “Turbolenza” - Vocabolario Accademia della Crusca, Venezia (1612)*

“And man shall be at peace when death removes him from the turbulence of this world and he comes to know eternal wellbeing”

First definition of the word “turbolenza” from the Accademia della Crusca Dictionary, Venice, Italy (1612)

*To our colleague and friend Tim (1966–2010)*

# Preface 2011

With the 4th ITI conference in the beautiful ancient town of Bertinoro, North Italy, 2010, the tradition of the interdisciplinary turbulence initiative (ITI) has been continued. About 100 researchers from about 20 different countries gathered in the hospitable centre of the University of Bologna to present the latest contributions in turbulence research. After an external peer review process the present 63 papers were collected for this forth issue on "progress in turbulence" dedicated to the memory of Prof. Tim Nickels. Shortly after giving an invited lecture at the 4th ITI conference, the turbulence community lost a world-class scientist, a friend and devoted family man.

Basic as well as applied research is driven by the rather notorious difficult and essentially unsolved problem of turbulence. In this collection of contributions clear progress can be seen in different aspects, ranging from new quality of numerical simulations to new concepts of experimental investigations and new theoretical developments. The importance of turbulence is shown for a wide range of applications including: combustion, energy, flow control, urban flows, are few examples found in this volume. A motivation this year was to bring fundamentals of turbulence in connection with renewable energy. This lead us to add a special topic relevant to the impact of turbulence on the wind energy conversion.

Beside all progress we have to realize that a general fundamental understanding of turbulence is still missing, even though new approaches are discovered and investigated. These new approaches often lead to new methods, which result in being very useful for other disciplines. Thus turbulence research has been a source of new scientific fields over the last decades. Nonlinear dynamics, chaos research, fractals and complexity may be taken as examples.

This span of research from pure mathematical analysis over turbulence physics to applied turbulence research has lead in the last decades to a broad diversification of turbulence research where contact between different sub-communities has sometimes been lost. It was in particular the latter drifting apart in the community that has

been the stimulation of the interdisciplinary turbulence initiative, which started in 1999 as cooperation between physicists and engineers working in turbulence funded by the German science foundation DFG. Based on the successful previous conferences, we will continue with this initiative for subsequent years with the 5th ITI Conference planned for September 2012.

The structure of the present book is as such that contributions have been bundled according to covering topics i.e. I Basic Turbulence Aspects, II Particle Laden Flows, III Modeling and Simulations, IV, Experimental Methods, V Special Flows, VI Atmospheric Boundary Layer, VII Boundary Layer, VIII Wind Energy and IX Convection.

At this point we would like to thank all authors for their contributions to this proceedings and the referees giving critical comments to the contributions and there with considerably raising the scientific quality. We would like to thank Thomas Ditzinger from Springer for his patience during the production of the book. Finally we gratefully acknowledge the staff of the University of Bologna and Olga Kelbin, George Khujadze, Andreas Rosteck for helping us to carry out this conference.

Martin Oberlack
Joachim Peinke
Alessandro Talamelli
Luciano Castillo
Michael Hölling
(Darmstadt, Oldenburg, Forli and Texas, 2012)

# Contents

## Session 1: Basic Turbulence Aspects

## Session 5: Special Flows



## Session 6: Atmospheric Boundary Layer

## Session 7: Boundary Layer

## Session 8: Wind Energy

## Session 9: Convection

# Session 1

# Basic Turbulence Aspects

# Scale-Energy Fluxes in Wall-Turbulent Flows

A. Cimarelli, E. De Angelis, and C.M. Casciola

**Abstract.** According to the Kolmogorov theory, the most important feature of high Reynolds number turbulent flows is the energy transfer from large to small scales. This energy cascade is believed to universally occur in a certain interval of scales, known as inertial range. This phenomenology has been shown to occur in a wide range of flows but not in wall-turbulence where a reverse cascade in the near-wall region is observed [1]. In order to analyse this new scenario, in the present work a study of a generalized Komogorov equation is performed. The results reveal an energy fluxes loop in the space of scales where the reverse cascade plays a central role. At the base of this phenomena it is found the anisotropic energy injection due to the action of the turbulent structures involved in the near-wall cycle. The data used for the analysis are obtained with a pseudo-spectral code in a channel at $Re_\tau = 550$. The computational domain is $8\pi h \times 2h \times 4\pi h$ with a resolution in the homogeneous directions of $\Delta x^+ = 13.5$ and $\Delta z^+ = 6.7$.

## 1 The Energy Transfer in Wall-Turbulence

The most important contribution to the description of the energy transfer mechanisms in turbulence is the Kolmogorov theory. Under the assumption of a statistical isotropic condition, this theory is an exact quantitative result obtained by the balance of the second order structure function, $\langle \delta u^2 \rangle$, where $\delta u_i = u_i(x_s + r_s) - u_i(x_s)$ is the fluctuating velocity increment and $\langle \cdot \rangle$ denotes ensamble average. Although this is a well known result it is useful to go back

A. Cimarelli · E. De Angelis
DIEM, Università di Bologna, Viale Risorgimento, 40136 Bologna, Italy
e-mail: andrea.cimarelli2@unibo.it, e.deangelis@unibo.it

C.M. Casciola
DIMA, Università di Roma "La Sapienza" Via Eudossiana 18, 00184 Roma, Italy
e-mail: carlomassimo.casciola@uniroma1.it

M. Oberlack et al. (Eds.): Progress in Turbulence and Wind Energy IV, SPPHY 141, pp. 3–6.
springerlink.com 

over its assumptions. The balance of $\langle \delta u^2 \rangle$, for small scales but sufficiently large so that the viscous diffusion processes may be neglected, reduces to the 4/5 law,

$$\langle \delta u_{||}^3 \rangle = -\frac{4}{5} \langle \epsilon \rangle r \tag{1}$$

where $||$ denotes longitudinal velocity increments and $\epsilon = \nu \left(\partial u_i \partial x_j\right) \left(\partial u_i \partial x_j\right)$ is the pseudo-dissipation. This relation establishes that the turbulent energy is transfered through the inertial range from large to small scales independently on the scale under consideration and with a constant rate proportional to the energy input/dissipation, $\langle \epsilon \rangle$. There is no direct energy injection and no direct energy extraction. This picture is believed to universally occur independently of the large-scale processess which feeds the turbulence, but fails in wall-turbulence where the interaction between anisotropic production and inhomogeneous spatial fluxes strongly modifies the energy cascade up to a reverse cascade in the near-wall region [1].

Wall-bounded turbulence is characterized by several processes which maybe thought as belonging to two different classes: phenomena which occur in physical space and phenomena which take place in the space of scales. The most significant aspect of the former is the spatial flux of turbulent kinetic energy and of the latter is the energy transfer among scales due to the coupling between eddies of different size. As a consequence, a full understanding of these phenomena requires a detailed description of the processes occurring simultaneously in physical and scale space. A tool for the study of these phenomena is the generalized form of the Kolmogorov equation [2]. This equation, specialized for a channel flow with a longitudinal mean velocity $U(y)$, reads,

$$\begin{aligned} &\frac{\partial \langle \delta u^2 \delta u_i \rangle}{\partial r_i} + \frac{\partial \langle \delta u^2 \delta U \rangle}{\partial r_x} + 2 \langle \delta u \delta v \rangle \left(\frac{dU}{dy}\right)^* + \frac{\partial \langle v^* \delta u^2 \rangle}{\partial Y_c} = \\ &\quad - 4 \langle \epsilon^* \rangle + 2\nu \frac{\partial^2 \langle \delta u^2 \rangle}{\partial r_i \partial r_i} - \frac{2}{\rho} \frac{\partial \langle \delta p \delta v \rangle}{\partial Y_c} + \frac{\nu}{2} \frac{\partial^2 \langle \delta u^2 \rangle}{\partial {Y_c}^2} \end{aligned} \tag{2}$$

where $^*$ denotes a mid-point average, i.e. $u_i^* = (u_i(x_s') + u_i(x_s))/2$ and $\langle \cdot \rangle$ denotes now average in the homogeneous directions. Equation 2 is written in a four dimensional space, $(r_x, r_y, r_z, Y_c)$, and involves a four dimensional energy fluxes vector field $\mathbf{\Phi} = (\Phi_{r_x}, \Phi_{r_y}, \Phi_{r_z}, \Phi_c)$,

$$\nabla \cdot \mathbf{\Phi}(\mathbf{r}, Y_c) = \xi(\mathbf{r}, Y_c) \tag{3}$$

where $\nabla \cdot$ is a four dimensional divergence, $\mathbf{\Phi}_r = (\Phi_{r_x}, \Phi_{r_y}, \Phi_{r_z}) = \langle \delta u^2 \delta \mathbf{u} \rangle - 2\nu \nabla_r \langle \delta u^2 \rangle$, $\Phi_c = \langle v^* \delta u^2 \rangle + 2 \langle \delta p \delta v \rangle / \rho - \nu d \langle \delta u^2 \rangle / 2 dY_c$ and $\xi = 2 \langle \delta u \delta v \rangle \left(dU/dy\right)^* - 4 \langle \epsilon^* \rangle$. This form allows us to appreciate the two scale-energy fluxes occuring in wall-flows, namely $\mathbf{\Phi}_r$ through the scales of motion and $\Phi_c$ in physical space. These fluxes assembled in the vector $\mathbf{\Phi}$ balance with a source term $\xi$ which accounts for the energy production and dissipation.

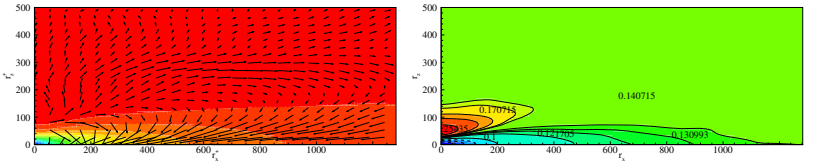


**Fig. 1** Scale-space behaviour at $Y_c^+ = 20$ of the energy fluxes vector $(\Phi_{r_x}, \Phi_{r_z})$ with contour levels of $\langle \delta u^2 \rangle$ (left) and contour levels of $\xi(r_x, r_z, |Y_c)$ (right).

When this term reaches a positive value, $\xi(\mathbf{r}, Y_c) > 0$, the energy injection via turbulent production exceeds the rate of energy dissipation. Therefore, the regions of the $(\mathbf{r}, Y_c)$-space where $\xi > 0$ can be thought as characterized by a scale-energy excess.

The phenomena of scale-energy excess is a peculiar aspect which characterizes wall-turbulent flows with respect to homogenous flows where the source term satisfies the constrain $\xi_{hom}(\mathbf{r}) \leq 0$. In homogeneous flows an excess of scale-energy cannot be observed. The energy transfer is initialized at the largest scales by production whose amount equals the energy dissipation, $\xi_{hom}(\mathbf{r}) = 0$ for $r \to \infty$. Then, out of the limit of large scales, the source term becomes negative, $\xi_{hom}(\mathbf{r}) < 0$, due to the monotonic decrease of the production moving to small scales, see Casciola et al. [3]. Whereas, in wall-turbulence there is not a balance between energy injection and dissipation due to the presence of the inhomogeneous spatial fluxes. Indeed, it is well known that turbulent production exceeds dissipation in the buffer layer leading to an excess of scale-energy $\xi(\mathbf{r}, Y_c) > 0$ at least for larger scales. This is a very important phenomena which strongly modifies the energy fluxes pattern of wall-turbulence from those usually observed in homogeneous flows. Equation 3 describes a vector field $\mathbf{\Phi}(\mathbf{r}, Y_c)$ where are present both energy source $(\xi(\mathbf{r}, Y_c) < 0)$ and sink $(\xi(\mathbf{r}, Y_c) > 0)$ regions in the $(\mathbf{r}, Y_c)$-space. As shown in figure 1, the energy fluxes follow a sort of loop in the space of scales. The fluxes first diverge from the energy source region feeding longer and wider turbulent fluctuations through a reverse cascade. Then, the fluxes converge to a classical forward cascade reaching the region of energy sink at the smallest dissipative scales. The energy source region and, therefore, the peak of energy production, take place deep inside the spectrum of scales, see figure 1. The energy is not introduced at the top of the spectrum and, therefore, there is not an isotropic recovery as expected in the Kolmogorov theory. The energy transfer is initialized at small scales and, diverging, leads to a strong reverse cascade. The location of the energy source region appears closely related to the action of the coherent structures involved in the near-wall cycle [4]. In particolar the spacing of this region suggest that this is presumably the imprint of the quasi-streamwise vortices. Indeed, most of the turbulent production of wall-turbulence is commonly associated to their action, see figure 2. Since the region of energy source is related to the streamwise vortices, the

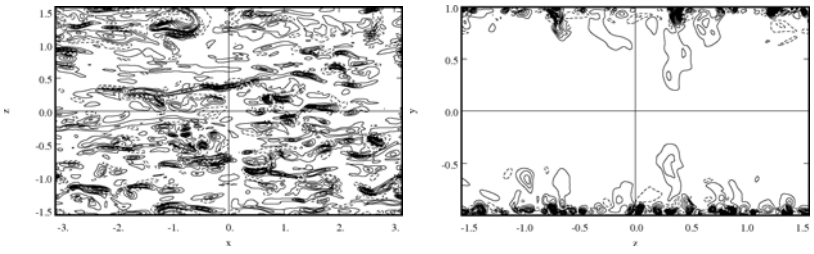


**Fig. 2** Isocontour of the istantaneous turbulent production occuring in a xz-plane at $Y_c^+ = 20$ (left) and in a yz-plane (right). The production pattern appears to be the imprint of the structures involved in the near-wall cycle.

generation of the streamwise velocity streaks is a result of the reverse energy cascade. In an energetic point of view, the whole near-wall cycle corresponds to an energy fluxes loop in the space of scales.

## 2 Conclusions

The present work has been devoted to the assessment of the energy fluxes in the space of scales of wall-turbulent flows. The analysis has shown an unexpected loop in the space of scales of the energy fluxes where a strong reverse cascade occurs. At the base of this phenomena has been found the presence of a peak of energy production in a small-scale region of the buffer layer which causes the divergence of the energy fluxes. This energy source region appears closely related to the dynamics of the quasi-streamwise vortices belonging to the near-wall cycle.

**Acknowledgements.** This work has been supported by the supercomputing center C.A.S.P.U.R. with a grant of computer time.

## References

1. Marati, N., Casciola, C.M., Piva, R.: Energy cascade and spatial fluxes in wall turbulence. J. Fluid Mech. 521 (2004)
2. Hill, R.J.: Exact second-order structure-function relationships. J. Fluid Mech. 468 (2002)
3. Casciola, C.M., Gualtieri, P., Benzi, R., Piva, R.: Scale-by-scale budget and similarity laws for shear turbulence. J. Fluid Mech. 476 (2003)
4. Jiménez, J., Pinelli, A.: The autonomous cycle of near-wall turbulence. J. Fluid Mech. 389 (1999)

# Conservation Laws of Helically Symmetric Flows and Their Importance for Turbulence Theory

O. Kelbin, A.F. Cheviakov, and M. Oberlack

**Abstract.** Our present understanding of statistical 3D turbulence dynamics in the large wave number limit (or small scales) largely relies on the dissipation of turbulent kinetic energy a quantity which is invariant under all symmetry groups of Navier-Stokes equations except the scaling groups. In turn, this implies Kolmogorov's sub-range theory and to a large part our understanding of energy transfer. On the other hand in 2D turbulence, which is translational invariant in one direction, the transfer mechanism among scales is rather different since the vortex stretching mechanism is non-existing. Instead, the scale determining key invariant is enstrophy: an area integral of the vorticity squared which is one of the infinite many integral invariants (Casimirs) of 2D inviscid fluid mechanics. Hence the basic transfer mechanisms between 2D and 3D turbulence are very different. To close this gap we consider flows with a helical symmetry which is a twist of translational and rotational symmetry. The resulting equations are "$2\frac{1}{2}$D" which means they have three independent velocity components though only two independent spatial variables. We presently show that in the inviscid limit the helically symmetric equations of motion admit a finite number of new non-trivial conservation laws comprising

- vorticity - though the basic vortex stretching mechanism is still active for helical flows and
- stream function even in a non-linear form clearly stating a non-local conservation laws since the stream-function is a line integral.

O. Kelbin · M. Oberlack
Chair of Fluid Dynamics, TU Darmstadt, Petersenstr. 30, 64287 Darmstadt, Germany

A.F. Cheviakov
Department of Mathematics and Statistics, University of Saskatchewan, Saskatoon, Canada

M. Oberlack
Center of Smart Interfaces, TU Darmstadt, Petersenstr. 32, 64287 Darmstadt, Germany

M. Oberlack
GS Computational Engineering, TU Darmstadt, Dolivostr. 15, 64293 Darmstadt, Germany

M. Oberlack et al. (Eds.): Progress in Turbulence and Wind Energy IV, SPPHY 141, pp. 7–10.
springerlink.com 

It is to be expected that the new conservation laws may give some deeper insight into turbulence dynamics and hence bridging 2D and 3D turbulence.

## 1 Mathematical Formulation of Helical Flows

We start with cylindrical coordinates $(r,\phi,z)$ and introduce helical coordinates $(r,\eta,\xi)$ defined by $\eta = a\phi - bz/r^2, \quad \xi = az + b\phi, \quad a,b \in \mathbb{R}, \quad a^2+b^2 > 0.$

A sketch of the coordinate system is depicted in figure 1. Here $h$ the pitch of the helix i.e for $a = 1$ we get $b = -h/(2\pi)$.

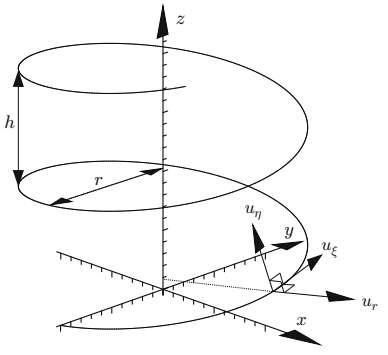


**Fig. 1** Helical coordinates with a line $\xi = const.$. $\eta = const.$ lines are orthogonal to the $\xi$-lines.

Considering a helically symmetry implies the key assumption that the velocity vector and pressure respectively write $\mathbf{u} = u_r(t,r,\xi)\mathbf{e}_r + u_\eta(t,r,\xi)\mathbf{e}_\eta + u_\xi(t,r,\xi)\mathbf{e}_\xi$ and $p = p(t,r,\xi)$ i.e. they are all independent of $\eta$.

The Euler equations in this helical notation become:

$$\frac{u_r}{r} + \frac{\partial u_r}{\partial r} + \frac{1}{B(r)}\frac{\partial u_\xi}{\partial \xi} = 0, \quad \text{(1a)}$$

$$\frac{\partial u_r}{\partial t} + u_r\frac{\partial u_r}{\partial r} + \frac{1}{B(r)}u_\xi\frac{\partial u_r}{\partial \xi} - \frac{B^2(r)}{r}\left(\frac{b}{r}u_\xi + a u_\eta\right)^2 + \frac{\partial p}{\partial r} = 0, \quad \text{(1b)}$$

$$\frac{\partial u_\eta}{\partial t} + u_r\frac{\partial u_\eta}{\partial r} + \frac{1}{B(r)}u_\xi\frac{\partial u_\eta}{\partial \xi} + \frac{a^2B^2(r)}{r}u_r u_\eta = 0, \quad \text{(1c)}$$

$$\frac{\partial u_\xi}{\partial t} + u_r\frac{\partial u_\xi}{\partial r} + \frac{u_\xi}{B(r)}\frac{\partial u_\xi}{\partial \xi} + \frac{2abB^2(r)}{r^2}u_r u_\eta + \frac{b^2B^2(r)}{r^3}u_r u_\xi + \frac{1}{B(r)}\frac{\partial p}{\partial \xi} = 0, \quad \text{(1d)}$$

with the metric term $B(r) = \frac{r}{\sqrt{a^2r^2+b^2}}$.

The latter equations, presented in primitive variables, may be written in two another formulations i.e. stream function formulation and vorticity variables. Due to

lake of space we do not specify the equations and limit ourselves to the description of the procedure how to obtain these equations. At first we introduce a stream function $\Psi = \Psi(t, r, \xi)$ such that

$$u_r = -\frac{1}{r}\frac{\partial \Psi}{\partial \xi}, \quad u_\xi = \frac{B(r)}{r}\frac{\partial \Psi}{\partial r} \tag{2a}$$

which solves (1a) and in a second step we eliminate the pressure $p$ via cross-differentiation and summation of (1b) and (1d). With this we obtain a PDE system of two equations for $\Psi$ and $u_\eta$.

In case of vorticity formulation we apply a curl operator $\omega = \nabla \times \mathbf{u}$ to the momentum equations in (1), which eliminates the pressure $p$ and we obtain 3 transport equations for the vorticity $\omega$. The definition of vorticity components is the following:

$$\omega_r = -\frac{1}{B(r)}\frac{\partial u_\eta}{\partial \xi}, \quad \omega_\xi = \frac{\partial u_\eta}{\partial r} + \frac{a^2 B^2(r)}{r} u_\eta \tag{3a}$$

$$\omega_\eta = -\frac{\partial u_\xi}{\partial r} - \frac{u_\xi}{r} + \frac{1}{B(r)}\frac{\partial u_r}{\partial \xi} + \frac{a^2 B^2(r)}{r} u_\xi - \frac{2abB^2(r)}{r^2} u_\eta. \tag{3b}$$

## 2 Conservation Laws

We seek for local conservation laws using the *direct method*. The idea behind it is that each equation of the system under investigation will be multiplied with a multiplier depending on all independent and dependent variables including their derivatives up to a given order. The Euler operator will be applied to this system which in turn determines the multipliers and hence leads to local conservation laws in divergence form (see [1])

$$\frac{\partial \Phi_t}{\partial t} + \frac{\partial \Phi_r}{\partial r} + \frac{\partial \Phi_\xi}{\partial \xi} = 0. \tag{4}$$

It can further be proven (see also [1]) that this is a necessary and sufficient condition for conservation laws. For brevity we subsequently only give the densities $\Phi_t$ for the three different systems and omit the fluxes:

- Primitive variables:

$$\Phi_t^{(1)} = \frac{1}{2} r \left( u_r^2 + u_\eta^2 + u_\xi^2 \right), \quad \Phi_t^{(2)} = \frac{r}{a} B \left( -\frac{b}{r} u_\eta + a u_\xi \right), \tag{5a}$$

$$\Phi_t^{(3)} = rF\left( \sqrt{a^2 r^2 + b^2}\, u_\eta \right), \quad \Phi_t^{(4)} = 0, \tag{5b}$$

  which include energy, momentum in $z$-direction, an arbitrary function of momentum in $\eta$-direction and, of course, conservation of mass which contains no time derivative.

- Stream function formulation:

$$\Phi_t^{(1)} = \frac{r}{2}u_\eta^2 + \frac{a^2r^2 - b^2}{2(a^2r^2+b^2)^2}\Psi\Psi_r - \frac{B^2}{2r}\Psi\Psi_{rr} - \frac{1}{2r}\Psi\Psi_{\xi\xi}, \tag{6a}$$

$$\Phi_t^{(2)} = -\frac{2bB}{a}u_\eta - \frac{4b^2B^2}{r^3}\Psi - r\Psi_{\xi\xi}, \quad \Phi_t^{(3)} = -\frac{G(t)}{r}\Psi_{\xi\xi}. \tag{6b}$$

- Vorticity formulation:

$$\Phi_t^{(1)} = \frac{b^2B(r)^4}{r^2}\xi\omega_r - \frac{ar^2B(r)}{2b}\omega_\eta, \quad \Phi_t^{(2)} = 0, \quad \Phi_t^{(3)} = H(t,r)\omega_r, \tag{7a}$$

$$\Phi_t^{(4)} = \left(a^2r^2 + 2b^2\right)B(r)^4\xi\omega_r + \frac{bB(r)r^2}{2a}\omega_\eta, \tag{7b}$$

$$\Phi_t^{(5)} = \frac{2abB(r)^4I(t)}{r^2}\xi\omega_r + B(r)I(t)\omega_\eta, \tag{7c}$$

$$\Phi_t^{(6)} = \left(-\frac{a^2B(r)^2}{r}J(t,r,\xi) + J(t,r,\xi)_r\right)B(r)\omega_r + J(t,r,\xi)_\xi\omega_\xi \tag{7d}$$

All the latter conserved quantities do not trivially relate to the classical conservation laws and may need special interpretation.

The analysis of the Navier-Stokes equations for all three formulations did not reveal new conservation laws. In case of primitive variables we obtain same fluxes as in (5) except $\Phi_t^{(1)}$, i. e. conserved quantities for Navier-Stokes equations are momentum in $z$-direction, an arbitrary function of momentum in $\eta$-direction and mass. The energy does not stay preserved. The conserved quantities for streamfunction and vorticity formulations also form a subset of the conserved quantities for Euler equations as is to be expected.

## Reference

1. Bluman, G.W., Cheviakov, A.F., Anco, S.C.: Applications of Symmetry Methods to Partial Differential Equations. Springer, Applied Mathematical Sciences, Vol. 168 (2010)

# Velocity/Pressure-Gradient Correlation Modelling for Improved Prediction of Reattachment and Relaxation

C. Lo, I. Vallet, and B.A. Younis

**Abstract.** The computation of complex flows with large separation is one of the numerous instances where second-moment closures outperform two-equations models. Previous studies with the Reynolds-stress model developed by Gerolymos-Vallet [3] (GV RSM) indicate that separation is quite accurately predicted, but also that there is room for improvement in the reattachment and relaxation region. Extensive testing suggests that the modelling of the pressure terms in the Reynolds-stress transport equations has the greatest impact on the prediction of both separation and reattachment. We propose a second-moment closure including a pressure-velocity gradient model with an additional term in the basis of the slow-part redistribution tensor proposed by Lumley [7] and a closure for the pressure-diffusion tensor which model directly the divergence of the pressure-velocity correlation. The present Reynolds-stress model is validated against a shock-wave/turbulent-boundary-layer interaction on a compression ramp and compared with two second-moment closures and the linear two-equations model of Launder-Sharma [5] (LS $k-\varepsilon$).

## 1 Introduction

The purpose of the present paper is to develop a second-moment closure, separately modelling the anisotropy of dissipation and redistribution (Eq. 1), maintaining the

C. Lo, Research Assistant
UPMC, case 161, 4 place Jussieu, 75005 Paris France
e-mail: celine.lo@upmc.fr

I. Vallet, Assistant Professor
UPMC, case 161, 4 place Jussieu, 75005 Paris France
e-mail: isabelle.vallet@upmc.fr

B. A. Younis, Professor
Dept. of Civil and Environmental Engineering, University of California,
Davis CA 95616, USA
e-mail: bayounis@ucdavis.edu

M. Oberlack et al. (Eds.): Progress in Turbulence and Wind Energy IV, SPPHY 141, pp. 11–15.
springerlink.com 

satisfactory prediction of separation of the GV RSM [3] and with a specific model for pressure diffusion term $d_{ij}^{(p)}$ (Eq. 2), which was shown in previous studies [8, 9] to improve the prediction of reattachment and relaxation.
The flow is modelled by the Favre-Reynolds-averaged Navier-Stokes equations [3, 10], coupled with the appropriate modelled turbulence-transport equations. The exact transport equations for the Favre-Reynolds-averaged Reynolds-stresses are

$$\underbrace{\frac{\partial \bar{\rho}\widetilde{u_i''u_j''}}{\partial t}+\frac{\partial(\bar{\rho}\widetilde{u_i''u_j''}\tilde{u}_\ell)}{\partial x_\ell}}_{\text{convection } C_{ij}}=\underbrace{\frac{\partial}{\partial x_\ell}(-\bar{\rho}\widetilde{u_i''u_j''u_\ell''}-\overline{p'u_j''}\delta_{i\ell}-\overline{p'u_i''}\delta_{j\ell}+\overline{u_i''\tau_{j\ell}'}+\overline{u_j''\tau_{i\ell}'})}_{\text{diffusion } d_{ij}=d_{ij}^{\mathrm{T}}+d_{ij}^{\mu}}$$

$$\underbrace{\left(-\bar{\rho}\widetilde{u_i''u_\ell''}\frac{\partial\tilde{u}_j}{\partial x_\ell}-\bar{\rho}\widetilde{u_j''u_\ell''}\frac{\partial\tilde{u}_i}{\partial x_\ell}\right)}_{\text{production } P_{ij}}+\underbrace{\overline{p'\left(\frac{\partial u_i''}{\partial x_j}+\frac{\partial u_j''}{\partial x_i}-\frac{2}{3}\frac{\partial u_k''}{\partial x_k}\delta_{ij}\right)}}_{\text{redistribution } \phi_{ij}}+\underbrace{\frac{2}{3}\overline{p'\frac{\partial u_k''}{\partial x_k}}\delta_{ij}}_{\phi_p\cong 0}$$

$$\underbrace{-\left(\overline{\tau_{j\ell}'\frac{\partial u_i''}{\partial x_\ell}}+\overline{\tau_{i\ell}'\frac{\partial u_j''}{\partial x_\ell}}\right)}_{\text{dissipation } \bar{\rho}\varepsilon_{ij}}+\underbrace{\left(-\overline{u_i''}\frac{\partial\bar{p}}{\partial x_j}-\overline{u_j''}\frac{\partial\bar{p}}{\partial x_i}+\overline{u_i''}\frac{\partial\bar{\tau}_{j\ell}}{\partial x_\ell}+\overline{u_j''}\frac{\partial\bar{\tau}_{i\ell}}{\partial x_\ell}\right)}_{\text{density fluctuation effects } K_{ij}\cong 0} \tag{1}$$

where the symbol $\breve{(.)}$ is used to denote a function of average quantities that is neither a Reynolds-averaged $\overline{(.)}$ nor a Favre-average $\widetilde{(.)}$, $(\cdot)''$ are Favre-fluctuations and $(\cdot)'$ are nonweighted-fluctuations [3]. Convection and production are exact terms whereas the diffusion due to turbulent transport $d_{ij}^{\mathrm{T}}=d_{ij}^{(u)}+d_{ij}^{(p)}$ and molecular viscosity $d_{ij}^{(\mu)}$, the pressure-strain correlation $\phi_{ij}$ and the dissipation $\bar{\rho}\varepsilon_{ij}$ terms require modelling. The turbulent-length scale was determined by solving the Launder-Sharma [5] modified dissipation-rate $\varepsilon^*=\varepsilon-2\breve{\nu}(\mathrm{grad}\sqrt{\mathrm{k}})^2$ transport-equation, where $\mathrm{k}=\widetilde{u_i''u_i''}/2$ is the turbulent-kinetic energy and $\varepsilon=\varepsilon_{ii}/2$ its dissipation-rate. $x_\ell$ are the Cartesian space coordinates, $u_i$ are the velocity components, $\rho$ is the density, $p$ is the pressure, $\tau_{ij}$ is the viscous stress tensor, and $\delta_{ij}$ is the Kronecker symbol.

## 2 Present Reynolds-Stress Model

We maintain, in the modelling approach the splitting of the velocity/pressure-gradient tensor $\Pi_{ij}=\phi_{ij}+d_{ij}^{(p)}$ into the pressure-diffusion term $d_{ij}^{(p)}=\partial_{x_\ell}(-\overline{u_i'p'}\delta_{j\ell}-\overline{u_j'p'}\delta_{i\ell})$ where $\overline{p'u_j'}$ is the pressure-velocity correlation, the redistribution term $\phi_{ij}$ and the pressure-dilation correlation $\phi_p$ which is neglected. In the present closure, the pressure-diffusion model $d_{ij}^{(p)}$ contains a Lumley-type [7] slow quasi-homogeneous term, with a slow and a rapid inhomogeneous terms containing grad $\varepsilon^*\otimes$ grad $\varepsilon^*$ and grad k $\otimes$ grad k respectively

$$\frac{d_{ij}^{(p)}}{\bar{\rho}} = C^{\text{SP1}} \frac{\mathrm{k}^3}{\varepsilon^3} \frac{\partial \varepsilon^*}{\partial x_i} \frac{\partial \varepsilon^*}{\partial x_j} + C^{\text{SP2}} \frac{\partial (\widetilde{u_m'' u_m'' u_j''} \delta_{i\ell} + \widetilde{u_m'' u_m'' u_i''} \delta_{j\ell})}{\partial x_\ell} + C^{\text{RP}} \frac{\mathrm{k}^2}{\varepsilon^2} \check{S}_{k\ell}\, a_{\ell k} \frac{\partial \mathrm{k}}{\partial x_i} \frac{\partial \mathrm{k}}{\partial x_j}$$

$$C^{\text{SP1}} = C^{\text{RP}} = -0.005;\ C^{\text{SP2}} = -0.022;\ a_{ij} = \frac{\widetilde{u_i'' u_j''}}{\mathrm{k}} - \frac{2}{3}\delta_{ij};\ \check{S}_{ij} = \tfrac{1}{2}\left(\frac{\partial \tilde{u}_i}{\partial x_j} + \frac{\partial \tilde{u}_j}{\partial x_i}\right) \quad (2)$$

The redistribution term $\phi_{ij}$, which is zero in $\mathrm{k}-\varepsilon$ models ($\phi_{\ell\ell} = 0$), is the most important term in second-moment closures. We propose, a formulation where $\phi_{ij}$ is modelled separately from the dissipation term $\bar{\rho}\varepsilon_{ij}$

$$\begin{aligned}
\phi_{ij} =& -C_\phi^{\text{SH1}} \bar{\rho} \varepsilon^* a_{ij} + C_\phi^{\text{SI1}} \frac{\varepsilon^*}{\mathrm{k}} \left[ \bar{\rho} \widetilde{u_n'' u_m''} e_n^{\text{I}} e_m^{\text{I}} \delta_{ij} - \tfrac{3}{2} \bar{\rho} \widetilde{u_n'' u_i''} e_n^{\text{I}} e_j^{\text{I}} - \tfrac{3}{2} \bar{\rho} \widetilde{u_n'' u_j''} e_n^{\text{I}} e_i^{\text{I}} \right] \\
& - C_\phi^{\text{SH2}} \bar{\rho} \frac{\mathrm{k}}{\varepsilon} \frac{\partial \mathrm{k}}{\partial x_\ell} \left[ a_{ik} \frac{\partial \widetilde{u_k'' u_j''}}{\partial x_\ell} + a_{jk} \frac{\partial \widetilde{u_k'' u_i''}}{\partial x_\ell} - \frac{2}{3} \delta_{ij} a_{mk} \frac{\partial \widetilde{u_k'' u_m''}}{\partial x_\ell} \right] \\
& + C_\phi^{\text{SI2}} \left[ \phi_{nm}^{\text{SH2}} e_n^{\text{I}} e_m^{\text{I}} \delta_{ij} - \tfrac{3}{2} \phi_{in}^{\text{SH2}} e_n^{\text{I}} e_j^{\text{I}} - \tfrac{3}{2} \phi_{jn}^{\text{SH2}} e_n^{\text{I}} e_i^{\text{I}} \right] \\
& - C_\phi^{\text{RH}} \left( P_{ij} - \tfrac{1}{3} \delta_{ij} P_{mm} \right) + C_\phi^{\text{RI}} \left[ \phi_{nm}^{\text{RH}} e_n^{\text{I}} e_m^{\text{I}} \delta_{ij} - \tfrac{3}{2} \phi_{in}^{\text{RH}} e_n^{\text{I}} e_j^{\text{I}} - \tfrac{3}{2} \phi_{jn}^{\text{RH}} e_n^{\text{I}} e_i^{\text{I}} \right]
\end{aligned} \quad (3)$$

where the first term of slow-part $\phi_{ij}^{\text{SH1}} + \phi_{ij}^{\text{SI1}}$ is function of the modified dissipation-rate $\varepsilon^*$ to reach easily the correct zero-value of the velocity/pressure-gradient tensor $\Pi_{ij}$ at the wall. The coefficients $C_\phi^{\text{SI1}}$, $C_\phi^{\text{SI2}}$ and $C_\phi^{\text{RI}}$ which mimic distance from the wall effects but without the use of any wall-topology-related parameters (such as geometric distance from the wall), were calibrated on the DNS basis of Gerolymos-Senechal-Vallet [2] in a fully developed turbulent plane channel flow ($Re_\tau = 180$). The unit-vector $\mathbf{e}^{\text{I}}$ which points in the the direction of inhomogeneity of the turbulent field was introduced [3] to replace the geometric normal to the wall. The rapid-part closure $\phi_{ij}^{\text{RH}} + \phi_{ij}^{\text{RI}}$ developed by Gerolymos-Vallet [3] was not modified in the present study.

## 3 Models Comparison on a Supersonic Compression Ramp

The present closure was assessed by comparison with available experimental data on the compression-ramp configuration (Fig. 1) studied by Ardonceau [1]. The computational method used to solve the compressible Navier-Stokes equations with the turbulence closure is described in [4]. The inflow conditions as well as the computational grid details are given in [10]. A second-moment closure, which corresponds to the GV RSM [3] with the homogeneous-rapid-redistribution coefficient $C_\phi^{\text{RH}}$ proposed by Launder-Shima [6] (hereafter GV–LS RSM), was developed to analyse the redistribution-tensor $\phi_{ij}$ influence. The linear LS $\mathrm{k}-\varepsilon$ closure and the GV–LS RSM are not able to predict the separation zone and as a consequence seem to give the best result in the reattachment region. On the contrary, the present closure and the GV RSM, which use the $C_\phi^{\text{RH}}$ developed by Gerolymos-Vallet [3], are in good agreement with experimental data. However the present RSM, which closes

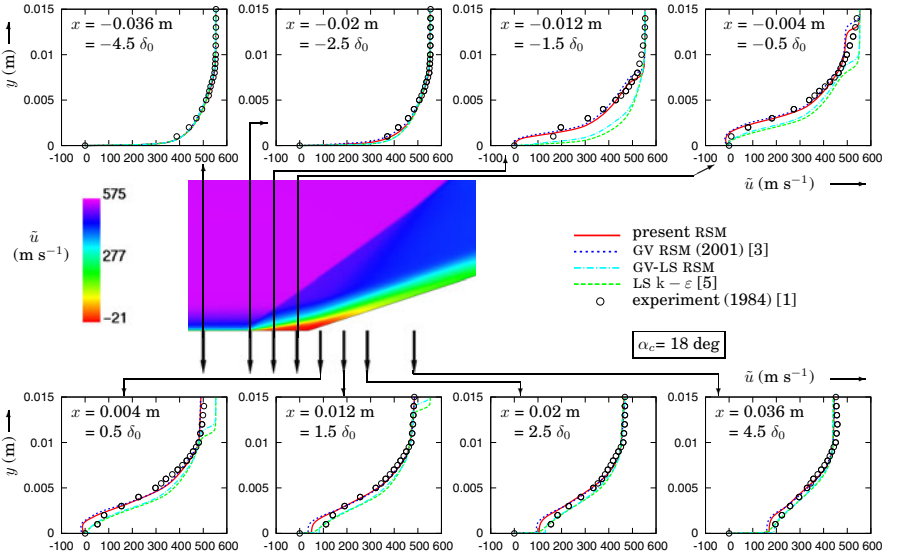


**Fig. 1** Comparison of grid-converged computations with measurements [1] of x-wise mean velocity at various axial stations, for the Ardonceau $\alpha = 18$ deg compression-ramp interaction ($M_\infty = 2.25$, $\mathrm{Re}_0 = 7 \times 10^3$).

the pressure-diffusion tensor, is slightly better after the corner ($x > 0$), especially in the relaxation region ($x \geq 2.5\delta_0$).

## 4 Conclusions

A new second-moment closure was assessed on a shock-wave/turbulent- boundary-layer interaction and compared with two other RSMs and a two-equations closure focusing on the prediction of the detachement and reattachement points. The predicting capability of full (differential) RSMs over a classical linear eddy-viscosity model is observed, confirming the study of Yakinthos [11] for attached flow in a 90-deg duct. The importance of the redistribution tensor to predict separation point is clearly identified while the pressure-diffusion closure slightly improve the prediction of the reattachement zone.

## References

1. Ardonceau, P.L.: The structure of turbulence in a supersonic shock-wave/boundary-layer interaction. AIAA J. 22(9), 1254–1262 (1984)
2. Gerolymos, G.A., Sénéchal, D., Vallet, I.: Performance of very-high-order upwind schemes for DNS of compressible wall-turbulence. Int. J. Num. Meth. Fluids 63, 769–810 (2010)

3. Gerolymos, G.A., Vallet, I.: Wall-normal-free near-wall Reynolds-stress closure for 3-D compressible separated flows. AIAA J. 39(10), 1833–1842 (2001)
4. Gerolymos, G.A., Vallet, I.: Mean-flow-multigrid for implicit Reynolds-stress-model computations. AIAA J. 43(9), 1887–1898 (2005)
5. Launder, B.E., Sharma, B.I.: Application of the energy dissipation model of turbulence to the calculation of flows near a spinning disk. Lett. Heat Mass Transf. 1, 131–138 (1974)
6. Launder, B.E., Shima, N.: 2-moment closure for the near-wall sublayer: Development and application. AIAA J. 27(10), 1319–1325 (1989)
7. Lumley, J.L.: Computational modeling of turbulent flows. Adv. Appl. Mech. 18, 123–176 (1978)
8. Sauret, E., Vallet, I.: Near-wall turbulent pressure diffusion modelling and influence in 3-D secondary flows. ASME J. Fluids Eng. 129(5), 634–642 (2007)
9. Vallet, I.: Reynolds-stress modelling of 3-D secondary flows with emphasis on turbulent diffusion closure. ASME J. Appl. Mech. 74(6), 1142–1156 (2007)
10. Vallet, I.: Reynolds-stress modelling of $M = 2.25$ shock-wave/turbulent-boundary-layer interaction. Int. J. Num. Meth. Fluids 56(5), 525–555 (2008)
11. Yakinthos, K., Vlahostergios, Z., Goulas, A.: Modeling the flow in a 90° rectangular duct using one Reynolds-stress and two eddy-viscosity models. Int. J. of Heat and Fluid Flow 29, 35–47 (2008)

# Turbulence without Richardson-Kolmogorov Cascade

J.C. Vassilicos and N. Mazellier

**Abstract.** We study turbulence generated by low-blockage space-filling fractal square grids [5]. This device creates a multiscale excitation of the fluid flow. Such devices have been proposed as alternative and complementary tools for the investigation of turbulence fundamentals, modelling and applications [3, 5, 6]. New insights on the fundamentals of homogeneous turbulence have been found, showing in particular that the small scales are not universal beyond small corrections caused by intermittency, finite Reynolds number and anisotropy. The unprecedented possibilities offered by these devices also open new attractive perspectives in applications involving mixing, combustion and flow management and control.

## 1 Introduction

A close approximation of homogeneous and isotropic turbulence can be achieved by means of grid-generated turbulence (see e.g. [1]). Even though its relevance to the study of turbulence fundamentals is clear, grid-generated turbulence produced by standard devices is often restricted to low Reynolds numbers. Deeper insights and understanding of turbulence physics (regarding, for instance, the mechanisms of interscale energy transfers) require new experimental approaches. Turbulence generated by multiscale/fractal grids is one such new approach [2]. Multiscale/fractal grids are new devices made from the superposition of a given pattern reproduced and multiplied at smaller scales (see Figure 1). Such a device is expected to excite a

J.C. Vassilicos
Turbulence, Mixing and Flow Control Group, Department of Aeronautics
Institute for Mathematical Sciences
Imperial College London, London, SW7 2BY, UK
e-mail: j.c.vassilicos@imperial.ac.uk

N. Mazellier
Institut PRISME, Université d'Orléans, 45072 Orléans, France
e-mail: nicolas.mazellier@univ-orleans.fr

M. Oberlack et al. (Eds.): Progress in Turbulence and Wind Energy IV, SPPHY 141, pp. 17–20.
springerlink.com 

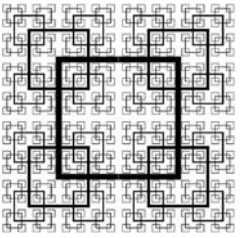

**Fig. 1** Typical example of a square multiscale/fractal grid. In this particular example, the grid has $N = 5$ fractal iterations.

broad range of turbulent scales, unlike standard regular grids. The turbulence generated by some such devices has already led to results which have shed serious doubt on the universality of the small-scale turbulence [3]. An attempt to account for some of these results has recently been made in terms of a single length-scale theory [7]. Here we report new insights on turbulence generated by space-filling fractal square grids and we discuss how the single-scale theory proposed in [7] accounts for our results.

## 2 Results

The streamwise evolution of the turbulence intensity measured along the centerline downstream of several fractal square grids is plotted in Figure 2. As reported in [2], we observe a protracted region closer to the grid where the turbulence builds-up until it reaches a maximum at $x = x_{peak}$ and then decays.

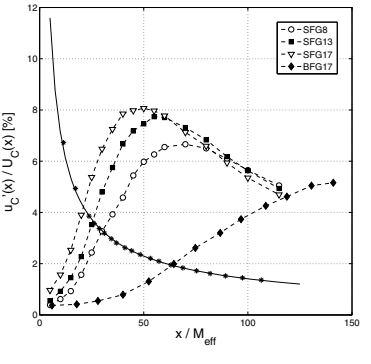


**Fig. 2** Turbulence intensity vs streamwise distance for four different fractal grids. See [4] for captions. The symbols (*) represent a standard regular grid.

The location of the turbulence peak is determined by the large-scale geometry of the fractal grids, but the observed fact that the turbulence is approximately homogeneous and isotropic shortly beyond $x_{peak}$ is determined by the multiple scales of the grid (see [4] for more details). It is worth noting that the turbulence levels achieved by means of fractal square grids are much higher than with standard regular grids (* symbols in Figure 2) and comparable to those reported for active grids [6].

A deeper investigation of the turbulent flow has been performed by studying the turbulent length-scales, in particular the integral length-scale $L_u$ (characteristic of the energy containing eddies) and the Taylor micro-scale $\lambda$ (characteristic of the smallest turbulent eddies). The ratio $L_u/\lambda$ computed for various inlet velocities $U_\infty$ in the decaying region (i.e. $x > x_{peak}$) of fractal square grid turbulence is plotted in Figure 3 as a function of the Taylor-based Reynolds number $Re_\lambda$. It turns out that the ratio $L_u/\lambda$ is independent of $Re_\lambda$ for a given $U_\infty$. This is a huge departure from the usual relationship found in standard fully developed turbulence, i.e. $L_u/\lambda \sim Re_\lambda$. This result seriously calls into question the statement that the dissipation constant and the interscale dynamics of small-scale turbulence are universal for large $Re_\lambda$.

Our results may be accounted for by means of a single length-scale self-preserving theory [7]. Starting from the spectral energy equation

$$\frac{\partial}{\partial t}E(k,t) = T(k,t) - 2\nu k^2 E(k,t), \tag{1}$$

and considering solutions of the form

$$E(k,t) = E_s(t,U_\infty,Re_0,*)f(kl(t),Re_0,*), \tag{2}$$
$$T(k,t) = T_s(t,U_\infty,Re_0,*)g(kl(t),Re_0,*), \tag{3}$$

where $Re_0 \equiv \frac{U_\infty t_0}{\nu}$ is the global Reynolds number based on the lateral thickness of the thickest bars on the fractal grid, $l(t) = l(t,Re_0,*)$ is the postulated unique characteristic length-scale of the turbulence, the argument $*$ represents any dependence on the initial/boundary conditions and the functions $f$ and $g$ are dimensionless. Combining Equations (1), (2) and (3) and extrapolating in a way explained in [4] (including an assumption of a $-5/3$ exponent at high Reynolds number) yields

$$E_u(k_x,x) = u'^2(x)L_0(k_xL_0)^{-5/3}H_u(k_xL_0Re_0^{-3/4}), \tag{4}$$
$$\varepsilon \approx 1.5u'^2U_\infty/x_{peak}, \tag{5}$$

for asymptotically high values of $Re_0$, where $L_0$ is the length of the longest bars on the grid. Our experimental results lend support to the single scale scaling of the energy spectrum as shown in Figure 4.

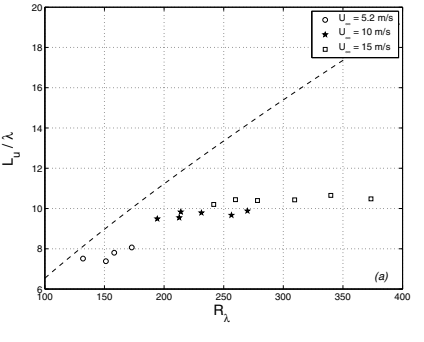


**Fig. 3** Turbulent length-scale ratio vs the Taylor-based Reynolds number. The dashed line represents values computed for standard fully developed turbulence, see [4].